

A modified Cuk DC-DC converter for DC microgrid systems

Andriazis Dahono, Arwindra Rizqiawan, Pekik Argo Dahono

School of Electrical Engineering and Informatics, Institute of Technology Bandung, Indonesia

Article Info

Article history:

Received Apr 22, 2020

Revised Jun 15, 2020

Accepted Jun 25, 2020

Keywords:

Cuk converter
DC-DC converter
Microgrid
Step-up converter

ABSTRACT

A new efficient step-up direct current- direct current (DC-DC) power converter that is suitable for DC microgrid systems is proposed in this paper. The proposed step-up DC-DC converter is derived from the conventional Cuk DC-DC power converter. Output voltage analysis that is useful to predict the conduction losses is presented. It is shown that the proposed step-up DC-DC converter is more efficient than the conventional DC-DC boost power converter. Current ripple analysis that is useful to determine the required inductors and capacitors is also presented. Experimental results are included to show the validity of the proposed step-up DC-DC power converter.

This is an open access article under the [CC BY-SA](https://creativecommons.org/licenses/by-sa/4.0/) license.



Corresponding Author:

Pekik Argo Dahono,
School of Electrical Engineering and Informatics,
Institute of Technology Bandung,
Ganesa St. No. 10, Bandung 40132, Indonesia.
Email: padahono@ieee.org

1. INTRODUCTION

Indonesia is an archipelago country with more than 17,000 islands. At present, the electrification ratio of the country is just about 97 % with many islands are still no access to electricity. Various programs have been established by the government to increase the electricity access especially in the remote areas or islands. As the locations are usually isolated, a microgrid system is suitable for these applications. If possible, the energy sources must be the locally available energy sources such as solar, wind, microhydro, or biomass.

Though the microgrid system can be implemented either as an alternating current (AC) or direct current (DC) microgrid, the DC system is desirable as there is no synchronization problem and easy load sharing. An example of DC microgrid system that has been developed is shown in Figure 1. The power sources can be photovoltaic (PV) modules, wind power, microhydro, or small internal combustion engines. A battery energy storage is used to store the energy from the sources. The DC grid voltage is 380-400 Vdc. Most of the load are lightings and electronic appliances. All DC-DC converters and inverters are constructed in one box and it is named as power unit as shown in Figure 2. The power unit, battery, and PV modules are located on the power pole. Instead of using power limiter, an energy limiter is installed for each customer.

Figure 2 shows that a DC-DC converter is used as an interface between the DC grid and DC energy sources and between the DC grid and battery energy storage. Various DC-DC power converters for these purposes have been proposed in the literature [1-20]. Though the DC-DC converter can be isolated or nonisolated, the nonisolated DC-DC converter is preferred because of power loss consideration. In addition to power loss consideration, the DC-DC power converters for this application have to produce low input and output current ripples. A low input current ripple is desirable in PV and battery applications to ensure a long

life operation. At present, the most commonly used DC-DC converter for PV power generation is the conventional nonisolated boost DC-DC power converter [1, 5]. This boost converter has a minimum number of passive and active devices. The conventional boost DC-DC converter has continuous input current and discontinuous output current.

This paper presents a simple and efficient step-up DC-DC power converter based on the modification of Cuk DC-DC power converter. As it is derived from Cuk DC-DC power converter, the input and output current ripples are small. Conduction losses and current ripple expressions are derived in this paper. It is shown that the conduction losses of the proposed converter are smaller than that of conventional DC-DC boost power converter. Several experimental results are included to show the validity of the proposed step-up DC-DC power converter.

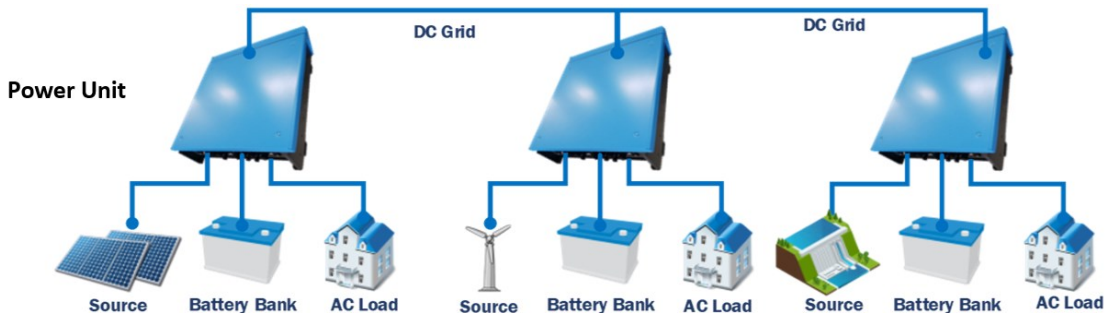


Figure 1. DC microgrid system

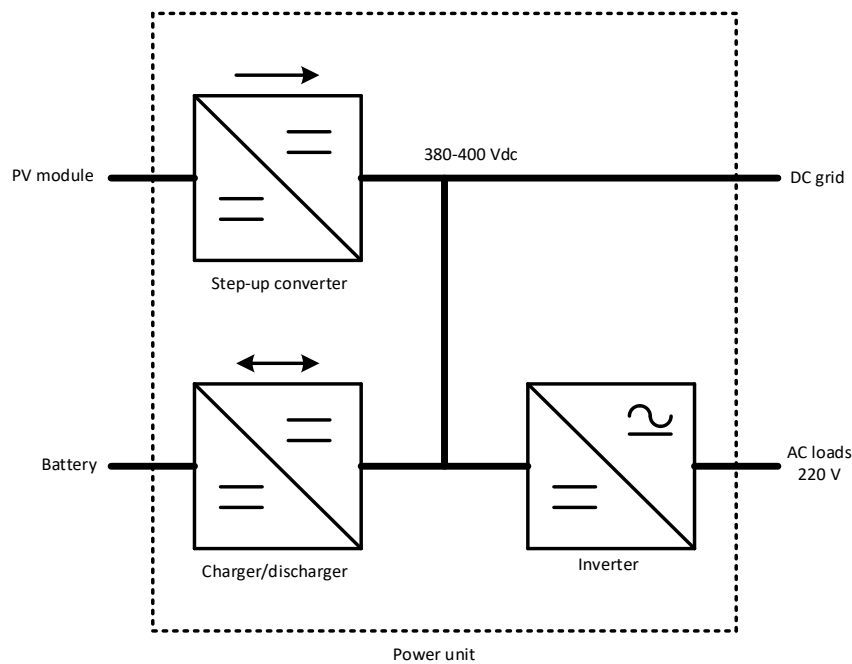


Figure 2. Power unit

2. MODIFIED CUK DC-DC POWER CONVERTER

The proposed DC-DC power converter is a modification result of Cuk DC-DC power converter [21]. The basic scheme of Cuk DC-DC power converter is shown in Figure 3. Though the active switching device is shown using metal oxide semiconductor field effect transistor (MOSFET), other type switching device can also be used. Under continuous conduction mode, it can be shown that the voltage ratio is;

$$\frac{\dot{v}_o}{E_d} = \frac{\alpha}{1-\alpha} \tag{1}$$

where $\alpha=T_{ON}/T_s$ is the duty cycle of transistor Q , T_{ON} is ON-period of transistor Q , and T_s is the switching period. The converter has a capability to produce an output voltage that is lower or higher than the DC input voltage. The power converter has continuous input and output currents with the associated low ripple content. Unfortunately, the polarity of the DC output voltage is reversed.

As it is shown in Figure 3, there is a third terminal that a load can be connected. The voltage ratio of the third terminal is;

$$\frac{\bar{v}_L}{E_d} = \frac{1}{1-\alpha} \tag{2}$$

If the load is connected to the third terminal, the load voltage is always higher than the input voltage. The voltage polarity of this third terminal is not reversed. For the same duty cycles, the voltage of third terminal is higher than the conventional load terminal. Fortunately, in our applications, the desired output voltage is always higher than the input voltage.

If the load is connected to the third terminal, then a new power converter as shown in Figure 4 (a) can be obtained. The load voltage is always higher than the input voltage as in the case of conventional boost DC-DC power converter. Different to the conventional one, however, the power converter in Figure 4 has a continuous output current with the associated low ripple content. If a bidirectional power flow is desired, then bidirectional switches as shown in Figure 4 (b) must be used. Depending on the power flow, the new power converter can be operated as a boost or buck DC-DC converter. The converter topology derivation method that is used in this paper has also been discussed in [22].

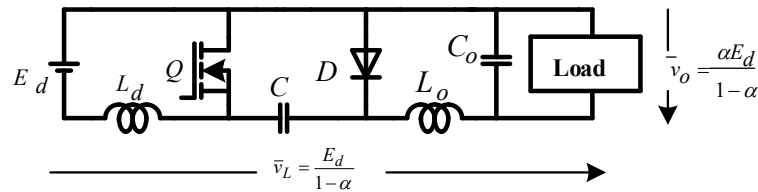


Figure 3. Modification of Cuk power converter

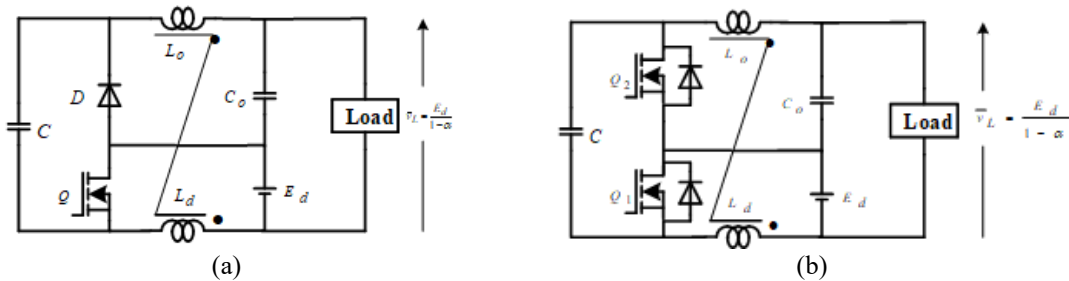


Figure 4. (a) Step-up and (b) bidirectional modified Cuk DC-DC converter

3. OUTPUT VOLTAGE ANALYSIS

In the previous section, the output voltage expressions have been derived by neglecting the voltage drops across inductors and switching power devices. In this section, output voltage analysis that takes into account the voltage drops across the inductors and switching devices is presented. Transistor Q and diode D in Figure 4 (a) work complementary. If transistor Q receives an ON (OFF) signal then diode D is turned OFF (ON). In order to make it more general, it is assumed that the voltage drops across the transistor and diode during conduction are;

$$v_Q = V_Q + R_Q i_Q \tag{3}$$

$$v_D = V_D + R_D i_D \tag{4}$$

where V_Q and V_D are the constant components, and R_Q and R_D are the resistive components of voltage drops and i_Q and i_D are currents of transistor and diode, respectively. The resistances of the inductors L_d and L_o are R_d and R_o , respectively. Capacitors C and C_o are assumed as ideal capacitors with no inductance nor resistance. The capacitor equivalent series resistances can be neglected in this analysis as the average value of capacitor current is zero during steady-state.

Figure 5 (a) shows the converter condition when transistor Q receives an ON signal. Under this condition, transistor Q is conducting the currents and diode D is turned OFF. Based on the circuit in Figure 5 (a), the following state space equation is obtained;

$$\begin{bmatrix} \frac{di_d}{dt} \\ \frac{di_o}{dt} \\ \frac{dv_C}{dt} \\ \frac{dv_o}{dt} \end{bmatrix} = \begin{bmatrix} -\frac{L_0(R_d+R_Q)}{\Delta} + \frac{MR_Q}{\Delta} & -\frac{L_0R_Q}{\Delta} + \frac{M(R_0+R_Q)}{\Delta} & -\frac{M}{\Delta} & \frac{M}{\Delta} \\ \frac{M(R_d+R_Q)}{\Delta} - \frac{L_dR_Q}{\Delta} & -\frac{L_d(R_0+R_Q)}{\Delta} + \frac{MR_Q}{\Delta} & \frac{L_d}{\Delta} & -\frac{L_d}{\Delta} \\ 0 & -\frac{1}{C} & 0 & 0 \\ 0 & \frac{1}{C_0} & 0 & 0 \end{bmatrix} \begin{bmatrix} i_d \\ i_o \\ v_C \\ v_o \end{bmatrix} + \begin{bmatrix} \frac{L_0}{\Delta}(E_d - V_Q) + \frac{M}{\Delta}V_Q \\ -\frac{M}{\Delta}(E_d - V_Q) - \frac{L_d}{\Delta}V_Q \\ 0 \\ -\frac{I_L}{C_0} \end{bmatrix} \quad (5)$$

where $\Delta=L_dL_0-M^2$ and M is the mutual inductance between inductors L_d and L_0 . Figure 5 (b) shows the converter state when transistor Q receives an OFF signal. Under this condition, the transistor Q is turned OFF and currents are flowing through the diode D . Based on the circuit in Figure 5 (b), the following is obtained;

$$\begin{bmatrix} \frac{di_d}{dt} \\ \frac{di_o}{dt} \\ \frac{dv_C}{dt} \\ \frac{dv_o}{dt} \end{bmatrix} = \begin{bmatrix} -\frac{L_0(R_d + R_D)}{\Delta} + \frac{MR_D}{\Delta} & -\frac{L_0R_D}{\Delta} + \frac{M(R_0 + R_D)}{\Delta} & -\frac{L_0}{\Delta} & \frac{M}{\Delta} \\ -\frac{L_dR_D}{\Delta} + \frac{M(R_d + R_D)}{\Delta} & -\frac{L_d(R_0 + R_D)}{\Delta} + \frac{MR_D}{\Delta} & \frac{M}{\Delta} & -\frac{L_d}{\Delta} \\ \frac{1}{C} & 0 & 0 & 0 \\ 0 & \frac{1}{C_0} & 0 & 0 \end{bmatrix} \begin{bmatrix} i_d \\ i_o \\ v_C \\ v_o \end{bmatrix} + \begin{bmatrix} \frac{L_0}{\Delta}(E_d - V_D) + \frac{M}{\Delta}V_D \\ -\frac{M}{\Delta}(E_d - V_D) - \frac{L_d}{\Delta}V_D \\ 0 \\ -\frac{I_L}{C_0} \end{bmatrix} \quad (6)$$

Transistor Q receives an ON signal during ON period and receives an OFF signal during OFF period. By taking the average of (5) and (6) over one switching period then the state-space average equation of the converter can be obtained [23]. If it is assumed that $L_d = L_0$, $R_d = R_0$, and $M = 0$, then the following steady-state equation is obtained;

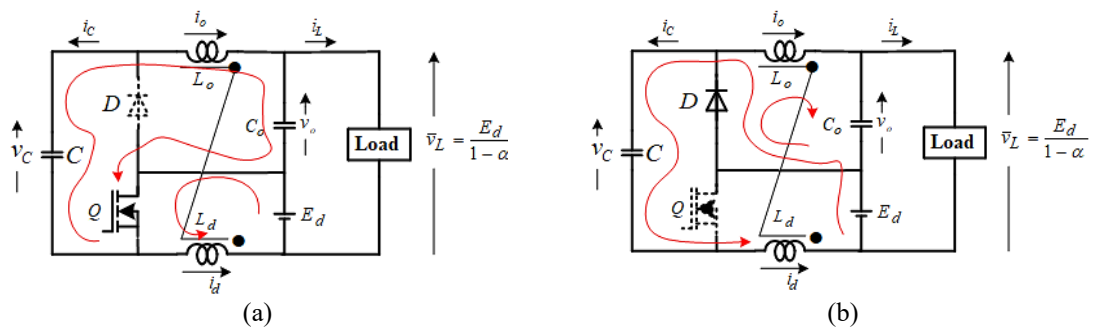


Figure 5. Converter condition when transistor Q receives an (a) ON-signal and (b) OFF-signal

$$0 = \begin{bmatrix} -\frac{L_d[R_d+R_Q\alpha+R_D(1-\alpha)]}{\Delta} & -\frac{L_d[R_Q\alpha+R_D(1-\alpha)]}{\Delta} & -\frac{L_d(1-\alpha)}{\Delta} & 0 \\ -\frac{L_d[R_Q\alpha+R_D(1-\alpha)]}{\Delta} & -\frac{L_d[R_d+R_Q\alpha+R_D(1-\alpha)]}{\Delta} & \frac{L_d\alpha}{\Delta} & -\frac{L_d}{\Delta} \\ \frac{1-\alpha}{c} & -\frac{\alpha}{c} & 0 & 0 \\ 0 & \frac{1}{c_0} & 0 & 0 \end{bmatrix} \begin{bmatrix} \bar{i}_d \\ \bar{i}_o \\ \bar{v}_C \\ \bar{v}_0 \end{bmatrix} + \begin{bmatrix} \frac{L_d[E_d-V_Q\alpha-V_D(1-\alpha)]}{\Delta} \\ -\frac{L_d[V_Q\alpha+V_D(1-\alpha)]}{\Delta} \\ 0 \\ -\frac{I_L}{c_0} \end{bmatrix} \quad (7)$$

Based on (7) we can obtain the following;

$$\bar{i}_d = \frac{\alpha}{1-\alpha} I_L \quad (8)$$

$$\bar{i}_o = I_L \quad (9)$$

$$\bar{v}_o = \frac{\alpha E_d}{1-\alpha} - \frac{V_Q\alpha+V_D(1-\alpha)}{1-\alpha} - \frac{R_d(1-2\alpha+2\alpha^2)+R_Q\alpha+R_D(1-\alpha)}{(1-\alpha)^2} I_L \quad (10)$$

The load voltage is;

$$\bar{v}_L = E_d + \bar{v}_o = \frac{E_d-V_Q\alpha-V_D(1-\alpha)}{1-\alpha} - \frac{R_d(1-2\alpha+2\alpha^2)+R_Q\alpha+R_D(1-\alpha)}{(1-\alpha)^2} I_L \quad (11)$$

In (10) is the output voltage expression of conventional Cuk DC-DC power converter and (11) is the modified Cuk DC-DC power converter. For the same output voltage, two times of the input voltage for example, the conventional Cuk DC-DC power converter needs duty cycle of 2/3 and the modified Cuk power converter needs duty cycle of half. By using the same method, the output voltage expression of conventional boost DC-DC power converter with the scheme as shown in Figure 6 can be obtained as;

$$\bar{v}_L = \frac{E_d-V_Q\alpha-V_D(1-\alpha)}{1-\alpha} - \frac{R_d+R_Q\alpha+R_D(1-\alpha)}{(1-\alpha)^2} I_L \quad (12)$$

Figure 7 shows the plots of voltage drop across the inductor resistance of conventional boost and proposed DC-DC power converters, as a function of duty cycle. This figure represents the conduction losses when the voltage drops across the switching devices are neglected. Though the number of inductor is double, the inductor losses are lower compared to the conventional boost DC-DC converter. It can be seen that the voltage drop in the proposed step-up DC-DC converter is lower than the conventional boost DC-DC converter. If the switching losses can be neglected, the conduction losses can be calculated as;

$$P_{loss} = E_d I_d - \bar{v}_L I_L \quad (13)$$

The input current is

$$I_d = \bar{i}_d + I_L \quad (14)$$

Substituting (8) into (14) the following is obtained

$$I_d = \frac{I_L}{1-\alpha} \quad (15)$$

Based on (10-13) and (15), the losses of converter is

$$P_{loss} = \frac{V_Q\alpha+V_D(1-\alpha)}{1-\alpha} I_L + \frac{R_d(1-2\alpha+2\alpha^2)+R_Q\alpha+R_D(1-\alpha)}{(1-\alpha)^2} I_L^2 \quad (16)$$

for conventional and modified Cuk DC-DC power converter, and

$$P_{loss} = \frac{V_Q\alpha+V_D(1-\alpha)}{1-\alpha} I_L + \frac{R_d+R_Q\alpha+R_D(1-\alpha)}{(1-\alpha)^2} I_L^2 \quad (17)$$

for conventional boost DC-DC power converter.

As it has been mentioned before, for the same output voltages, the duty cycle of modified Cuk DC-DC power converter is lower than the conventional one. Thus, the losses in modified Cuk DC-DC power converter is lower than the conventional ones. In (16, 17) show that for the same output voltages, the power loss in modified Cuk DC-DC power converter is lower than the conventional boost DC-DC power converter.

The reason why the inductor losses in modified Cuk DC-DC power converter are lower than the inductor losses in conventional boost DC-DC power converter can be explained as follows:

- All source current is flowing through the inductor of boost DC-DC converter.
- Currents through inductors L_d and L_o of modified Cuk DC-DC power converter are lower than the inductor current in conventional boost DC-DC power converter.

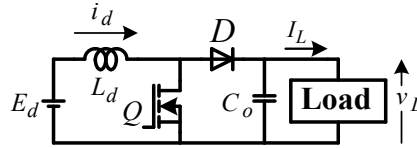


Figure 6. Conventional boost DC-DC power converter

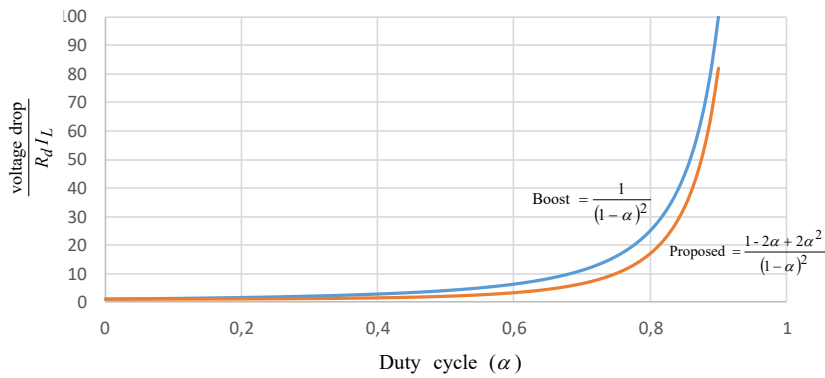


Figure 7. Voltage drop comparison

4. CURRENT RIPPLE ANALYSIS

In the following analysis, it is assumed that the inductor currents are continuous. Moreover, it is assumed that the voltage across the capacitor C is not changing so much in one switching period. Based on Figure 4 (a), the following can be obtained;

$$\begin{bmatrix} L_d & M \\ M & L_o \end{bmatrix} \begin{bmatrix} \frac{di_d}{dt} \\ \frac{di_o}{dt} \end{bmatrix} = \begin{bmatrix} E_d - v_Q \\ v_D - v_o \end{bmatrix} \tag{18}$$

where v_Q and v_D are voltages across transistor Q dan diode D , respectively, and M is the mutual inductance between L_d and L_o . The currents and voltages can be divided into the average and ripple components as the followings:

$$i_d = I_d + \tilde{i}_d \tag{19}$$

$$i_o = I_o + \tilde{i}_o \tag{20}$$

$$v_Q = V_Q + \tilde{v}_Q \tag{21}$$

$$v_D = V_D + \tilde{v}_D \tag{22}$$

$$v_o = V_o + \tilde{v}_o \tag{23}$$

where bar and tilde indicate average and ripple components, respectively. If (19-23) are substituted into (18) then the current ripple components can be obtained

$$\begin{bmatrix} L_d & M \\ M & L_o \end{bmatrix} \begin{bmatrix} \frac{d\tilde{i}_d}{dt} \\ \frac{d\tilde{i}_o}{dt} \end{bmatrix} = \begin{bmatrix} -\tilde{v}_Q \\ \tilde{v}_D - \tilde{v}_o \end{bmatrix} \quad (24)$$

Based on (24) the followings are obtained:

$$\tilde{i}_d = \frac{L_o}{\Delta} \int (-\tilde{v}_Q) dt - \frac{M}{\Delta} \int (\tilde{v}_D - \tilde{v}_o) dt + C_1 \quad (25)$$

$$\tilde{i}_o = \frac{L_d}{\Delta} \int (\tilde{v}_D - \tilde{v}_o) dt - \frac{M}{\Delta} \int (-\tilde{v}_Q) dt + C_2 \quad (26)$$

where C_1 and C_2 constants of integration. If it is assumed that the ripple component of switch voltage is much higher than the capacitor voltage ripple,

$$\tilde{v}_D \gg \tilde{v}_o \quad (27)$$

Then (25) and (26) can be approximated as;

$$\tilde{i}_d = \frac{L_o}{\Delta} \int (-\tilde{v}_Q) dt - \frac{M}{\Delta} \int \tilde{v}_D dt + C_1 \quad (28)$$

$$\tilde{i}_o = \frac{L_d}{\Delta} \int \tilde{v}_Q dt - \frac{M}{\Delta} \int (-\tilde{v}_Q) dt + C_2 \quad (29)$$

Based on (21-22), the ripple voltages of transistor are;

$$\tilde{v}_{Q1} = v_{Q1} - V_{Q1} \quad (30)$$

$$\tilde{v}_D = v_D - V_D \quad (31)$$

where,

$$V_Q = E_d \quad (32)$$

$$V_D = V_o = \frac{\alpha}{1-\alpha} E_d \quad (33)$$

when transistor Q receives an ON signal;

$$v_Q = 0 \quad (34)$$

$$v_D = \tilde{v}_C = \frac{E_d}{1-\alpha} \quad (35)$$

Thus, the current ripple expressions when transistor Q receives an ON signal are,

$$\tilde{i}_d = \frac{L_o - M}{\Delta} \int E_d dt + C_1 \quad (36)$$

$$\tilde{i}_o = \frac{L_d - M}{\Delta} \int E_d dt + C_2 \quad (37)$$

When transistor Q receives an OFF signal, the transistor voltages are,

$$v_Q = \tilde{v}_C = \frac{E_d}{1-\alpha} \quad (38)$$

$$v_D = 0 \quad (39)$$

thus, the current ripple expressions when transistor Q receives an OFF signal are,

$$\tilde{i}_d = -\frac{L_o - M}{\Delta} \int \frac{\alpha E_d}{1-\alpha} dt + C_3 \quad (40)$$

$$\tilde{i}_o = -\frac{L_d - M}{\Delta} \int \frac{\alpha E_d}{1-\alpha} dt + C_4 \quad (41)$$

where C_3 and C_4 are constants of integration. These constants can be determined based on the facts that:

- Average value of current ripple over one switching period is zero.
- Initial value of current ripple during ON period is the final value of the current ripple during OFF period. Similarly, the initial value of current ripple during OFF period is the final value of current ripple during ON period.

Based on the above analysis, the current ripple expression in one switching period can be written as;

$$\tilde{i}_d = \frac{E_d(L_o-M)}{\Delta} \begin{cases} -\frac{T_{ON}}{2} + (t - t_o) & \text{for } t_o \leq t \leq t_2 \\ \frac{\alpha}{1-\alpha} \frac{T_{OFF}}{2} - \frac{\alpha}{1-\alpha} (t - t_2) & \text{for } t_2 \leq t \leq t_4 \end{cases} \quad (42)$$

$$\tilde{i}_o = \frac{E_d(L_d-M)}{\Delta} \begin{cases} -\frac{T_{ON}}{2} + (t - t_o) & \text{for } t_o \leq t \leq t_2 \\ \frac{\alpha}{1-\alpha} \frac{T_{OFF}}{2} - \frac{\alpha}{1-\alpha} (t - t_2) & \text{for } t_2 \leq t \leq t_4 \end{cases} \quad (43)$$

Figure 8 shows the current ripples over one switching period. The rms values of current ripple can be determined as;

$$\tilde{I}_d = \left[\frac{1}{T_s} \int_{t_o}^{t_o+T_s} \tilde{i}_d^2 dt \right]^{1/2} \quad (44)$$

$$\tilde{I}_o = \left[\frac{1}{T_s} \int_{t_o}^{t_o+T_s} \tilde{i}_o^2 dt \right]^{1/2} \quad (45)$$

Based on (44, 45) the followings are obtained;

$$\tilde{I}_d = \frac{L_o-M}{2\sqrt{3}\Delta} \frac{\alpha E_d}{f_s} \quad (46)$$

$$\tilde{I}_o = \frac{L_d-M}{2\sqrt{3}\Delta} \frac{\alpha E_d}{f_s} \quad (47)$$

In (46, 47) show that the mutual inductance between the two inductors can be used to reduce the inductor current ripples. Based on the circuit in Figure 4, we can obtain the capacitor current as;

$$i_c = \begin{cases} -i_o & \text{for } t_o \leq t \leq t_o + T_{ON} \\ i_d & \text{for } t_o + T_{ON} \leq t \leq t_o + T_s \end{cases} \quad (48)$$

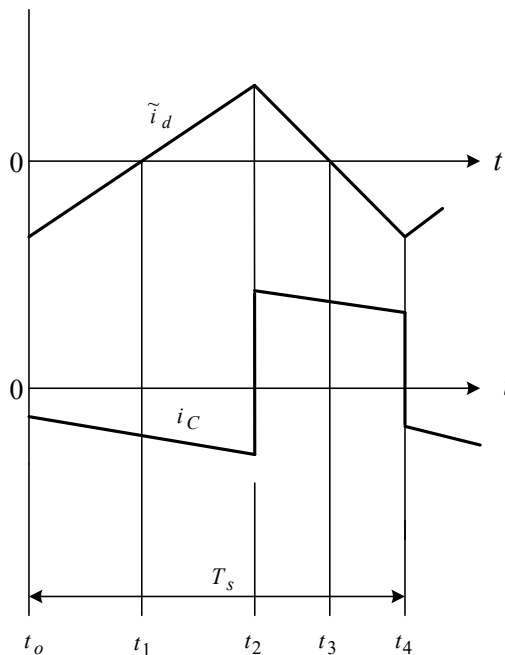


Figure 8. Converter current ripples over one carrier period

Figure 8 shows the capacitor current waveform. By neglecting the ripple components of i_o and i_d , the rms value of capacitor current is;

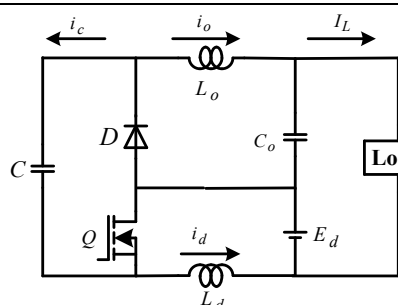
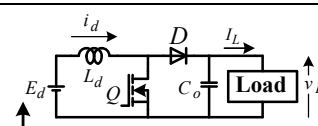
$$I_C = I_L \left(\frac{\alpha}{1-\alpha} \right)^{1/2} \quad (49)$$

In the proposed converter, therefore, a capacitor with a large current ripple rating is required. It can be seen that the capacitor current ripple cannot be reduced by increasing the switching frequency.

5. COMPARATIVE EVALUATION

In order to know the advantages and disadvantages of the proposed DC-DC converter, the performance of the proposed converter is compared to the conventional boost DC-DC power converter. The comparison is summarized in Table 1. In this comparison, the two inductors of modified Cuk DC-DC power converter are assumed equal with no mutual coupling.

Compared to the conventional boost DC-DC power converter, the proposed converter has the lowest conduction losses and lowest output capacitor current ripple. The reason why the inductor losses of modified Cuk DC-DC power converter are lower than the conventional boost DC-DC power converter can be seen from the inductor current expressions in Table 1. The inductor currents of modified Cuk DC-DC power converter are lower than the inductor current in conventional boost DC-DC converter. Thus, the efficiency of the proposed converter is the highest as the switching losses are almost the same. The disadvantage of the proposed converter is the need of a capacitor with a high current ripple rating. The use of film capacitor is preferred in this application. The two inductors can be integrated in one core so that the volume can be minimized. It should be noted that the proposed DC-DC power converter is a fourth-order converter and, therefore, the control is more difficult than the conventional boost DC-DC power converter. Various control methods for high-order DC-DC power converters were reported in [24-28].

| Table 1. Performance comparison | | |
|---------------------------------|---|---|
| | Modified Cuk | Conventional Boost |
| Circuit |  |  |
| Passive components | Two inductors and two capacitors | One inductor and one capacitor |
| Active components | One transistor, one diode | One transistor, one diode |
| Output voltage | $\bar{v}_L = \frac{E_d - V_Q \alpha - V_D (1 - \alpha)}{R_d (1 - 2\alpha + 2\alpha^2) + R_Q \alpha + R_D (1 - \alpha)} I_L$ | $\bar{v}_L = \frac{E_d - V_Q \alpha - V_D (1 - \alpha)}{R_d + R_Q \alpha + R_D (1 - \alpha)} I_L$ |
| Source current ripple | $\tilde{I}_d = \frac{1}{2\sqrt{3}} \frac{\alpha E_d}{L_d f_s}$ | $\tilde{I}_d = \frac{1}{2\sqrt{3}} \frac{\alpha E_d}{L_d f_s}$ |
| Output capacitor current ripple | $\tilde{I}_o = \frac{1}{2\sqrt{3}} \frac{\alpha E_d}{L_o f_s}$ | $\tilde{I}_o = I_L \left(\frac{\alpha}{1 - \alpha} \right)^{1/2}$ |
| Transfer capacitor current | $I_C = I_L \left(\frac{\alpha}{1 - \alpha} \right)^{1/2}$ | NA |
| Average input inductor current | $I_d = \frac{\alpha I_L}{1 - \alpha}$ | $I_d = \frac{I_L}{1 - \alpha}$ |
| Average output inductor current | $I_o = I_L$ | NA |

6. EXPERIMENTAL RESULTS

A small experimental system as the one shown in Figure 4 (b) was constructed. In this experiment, two power MOSFETs were used as switching devices. Uncoupled two equal inductors of 2.2 mH were used as L_d and L_o . The switching frequency can be varied from 1 kHz up to 20 kHz. The capacitance C is 220 uF and

the capacitance C_o is 330 μF . The DC source is obtained from a DC power supply that is maintained constant at 36 Vdc. The load is a constant resistance of 100 Ohm.

Figure 9 shows the output voltage as the function of duty cycle. Ideal curve is the calculated results when the voltage drops across the switching devices and inductors are neglected. The nonideal curve is calculated results when the voltage drops are taken into account as given by (9). Measurements were conducted under two switching frequencies. Measurement results are indicated by small square and circle. It can be seen that the derived expression is accurate in predicting the output voltage.

Figure 10 shows the experimental and calculated results of current ripple through inductor L_o of modified Cuk DC-DC power converter. Very good agreement between calculated and experimental results can be appreciated. Similar results are obtained for current ripple through inductor L_d . Similar to other DC-DC power converters, the current ripple can be reduced further by multiphasing technique.

Figure 11 shows the efficiency of modified Cuk DC-DC power converter when the duty cycle is changed. The load resistance during this experiment was constant. As it is predicted, the efficiency is higher when the duty cycle is small. The efficiency can be increased by reducing the resistances of the inductors. It should be noted that this efficiency is higher than the conventional boost DC-DC power converter.

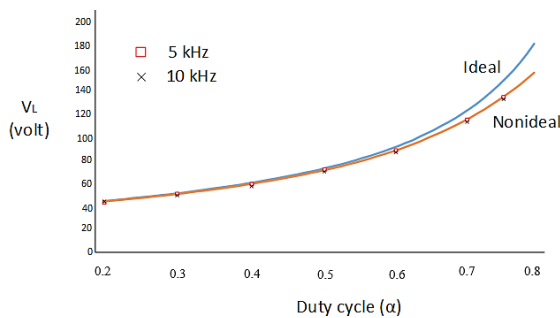


Figure 9. Output voltage as a function of duty cycle of modified Cuk DC-DC power converter

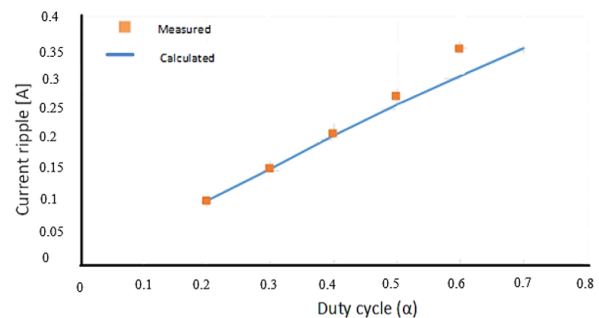


Figure 10. Inductor current ripple of modified Cuk DC-DC power converter

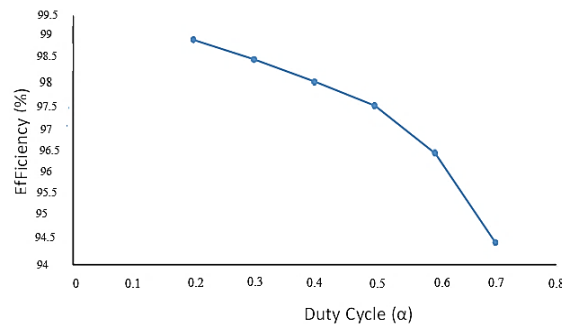


Figure 11. Efficiency of modified Cuk DC-DC power converter

7. CONCLUSION

An efficient step-up DC-DC power converter based on the modification of Cuk DC-DC power converter that is suitable for DC microgrid systems has been proposed. The conduction losses of the proposed converter are lower than the conventional boost DC-DC power converter. Analysis of output voltage and inductor current ripple that useful in converter design is presented. Experimental results have verified the analysis given in this paper. Practical industrial prototype of the proposed converter is in progress and will be reported in the future occasion.

ACKNOWLEDGEMENTS

The authors wish to thank PT. LEN (Persero) and LPDP for providing research funds of this work. This paper is dedicated to the anniversary of 100-year engineering education in Indonesia.

REFERENCES

- [1] Y. Huang, *et al.*, "Survey of the Power Conditioning System for PV Power Generation," *IEEE Power Electron. Spec. Conf. Rec.*, pp. 3257-3262, 2006.
- [2] E. Roman, *et al.*, "Intelligent PV Module for Grid-Connected PV Systems," *IEEE Trans. Ind. Electron.*, vol. 53, no. 4, pp. 1066-1073, 2006.
- [3] A. Bratcu, *et al.*, "Cascaded DC-DC Converter Photovoltaic Systems: Power Optimization Issues," *IEEE Trans. Ind. Electron.*, vol. 58, no. 2, pp. 403-411, 2011.
- [4] B. Liu, S. Duan, and T. Cai, "Photovoltaic DC-Building-Module-Based BIPV System – Concept and Design Considerations," *IEEE Trans. Power Electron.*, vol. 26, no. 5, pp. 1418-1429, 2011.
- [5] E. Cadaval, *et al.*: 'Grid-Connected Photovoltaic Generation Plants', *IEEE Ind. Electr. Mag.*, pp. 7-20, 2013.
- [6] D. Meneses, *et al.*, "Review and Comparison of Step-Up Transformerless Topologies for Photovoltaic AC-Module Application", *IEEE Trans. Power Electron.*, vol. 28, no. 6, pp. 3649-3663, 2013.
- [7] H. Bergveld, *et al.*, "Module-Level DC/DC Conversion for Photovoltaic Systems: The Delta-Conversion Concept," *IEEE Trans. Power Electron.*, vol. 28, no. 4, pp. 2005-2013, 2013.
- [8] M. Kasper, D. Bortis, and J. Kolar, "Classification and Comparative Evaluation of PV Panel-Integrated DC-DC Converter Concepts," *IEEE Trans. Power Electr.*, vol. 29, no. 4, 2014, pp. 2511-2526.
- [9] S. Kouro, *et al.*, "Grid-Connected Photovoltaic Systems," *IEEE Ind. Electr. Mag.*, pp. 47-61, 2015.
- [10] Y. Yang, A. Sangwongwanich, and F. Blaabjerg, "Design for Reliability of Power Electronics for Grid-Connected Photovoltaic Systems," *CPSS Trans. Power Electr. Appl.*, vol. 1, no. 1, pp. 92-103, 2016.
- [11] P. Shenoy, *et al.*, 'Differential Power Processing for Increased Energy Production and Reliability of Photovoltaic Systems', *IEEE Trans. Power Electron.*, Vol. 28, No. 6, June 2013, pp. 2968-2979.
- [12] M. Agamy, *et al.*, "An Efficient Partial Power Processing DC/DC Converter for Distributed PC Architectures," *IEEE Trans. Power Electron.*, vol. 29, no. 2, pp. 674-686, 2014.
- [13] H. Zhou, J. Zhao, and Y. Han, "PV Balancers: Concept, Architectures, and Realization," *IEEE Trans. Power Electron.*, vol. 30, no. 7, pp. 3479-3487, 2015.
- [14] K. Kim, P. Shenoy, and P. Krein, "Converter Rating Analysis for Photovoltaic Differential Power Processing Systems," *IEEE Trans. Power Electron.*, vol. 30, no. 4, pp. 1987-1997, 2015.
- [15] J. Zapata, *et al.*, "Partial Power DC-DC Converter for Photovoltaic Microinverter," *Proc. IEEE Ind. Electron. Conf.*, pp. 6740-6745, 2016.
- [16] R. Aprilianto, Subiyanto, and T. Sutikno, 'Modified SEPIC Converter Performance for Grid-connected PV Systems under Various Conditions,' *TELKOMNIKA Telecommunication, Computing, Electronics and Control*, vol. 16, no. 6, pp. 2943-2953, 2018.
- [17] G. Adams, *et al.*, "Review of technologies for DC grids – power conversion, flow control and protection," *IET Power Electron.*, vol. 12, no. 8, pp. 1851-1877, 2019.
- [18] A. Andrade, L. Schuch, and M. Martins, "Analysis and Design of High-Efficiency Hybrid High Step-Up DC-DC Converter for Distributed PV Generation Systems," *IEEE Trans. Ind. Electron.*, vol. 66, no. 5, pp. 3860-3868, 2019.
- [19] K. Nathan, *et al.*, "A New DC-DC Converter for Photovoltaic Systems: Coupled-Inductors Combined Cuk-SEPIC Converter," *IEEE Trans. Energy Conv.*, vol. 34, no. 1, pp. 191-201, 2019.
- [20] P.A. Dahono, 'Derivation of High Voltage-Gain Step-Up DC-DC Power Converters', *International Journal Electrical Engineering and Informatics*, vol. 11, no. 2, pp. 236-251, 2019.
- [21] S. Cuk and R. Middlebrook, "A New Optimum Topology Switching DC-DC Converter," *IEEE Power Electron. Spec. Conf. Rec.*, pp. 160-179, 1977.
- [22] B. Williams, "Basic DC-to-DC Converters," *IEEE Trans. Power Electron.*, vol. 23, no. 1, pp. 387-401, 2008.
- [23] R. Middlebrook and S. Cuk, "A General Unified Approach to Modelling Switching Converter Power Stages," *IEEE Power Electron. Spec. Conf. Rec.*, pp. 18-34, 1976.
- [24] J. Majo, *et al.*, "Large-Signal Feedback Control of a Bidirectional 1 Coupled-Inductor Cuk Converter," *IEEE Trans. Ind. Electron.*, vol. 39, no. 5, pp. 429-436, 1992.
- [25] Y. Liu, P. Sen, and S. Huang, "Function Control-A Novel Strategy to Achieve Improved Performance of the DC-to-DC Switching Regulators," *IEEE Trans. Ind. Electron.*, vol. 42, no. 2, pp. 186-191, 1995.
- [26] K. Smedley and S. Cuk, "Dynamics of One-Cycle Controlled Cuk Converters," *IEEE Trans. Power Electron.*, vol. 10, no. 6, pp. 634-639, 1995.
- [27] C. Chan, "Comparative study of current-mode controllers for a high-order boost DC-DC converter," *IET Power Electron.*, vol. 7, no. 1, pp. 237-243, 2013.
- [28] Y. Li, P. Jia, and T. Zheng, "Research on input-voltage feedforward control for high-order converter topologies," *IET Power Electron.*, vol. 7, no. 11, pp. 2778-2790, 2014.